

Metallicity of Ultrathin Metal Layers

ROBERT GOMER

Department of Chemistry and The James Franck Institute, The University of Chicago, Chicago, Illinois 60637

Received December 11, 1995

Introduction

Ultrathin metal films, one to several atomic layers in thickness, have attracted considerable attention in recent years. Apart from their morphology and growth modes on metal or semiconductor substrates and their catalytic and chemisorptive properties for which a considerable literature now exists,^{1,2} their electronic properties and specifically the question of whether they are still metallic are of considerable theoretical interest since such layers can begin to simulate two-dimensional systems. Given the voracity of the microelectronics industry for ever smaller devices, these questions may also turn out to be of technological importance.

This Account will first describe in elementary terms what is meant by metallicity and point out why ultrathin metal layers might not be metallic. Experimentally accessible criteria of metallicity will then be discussed, with emphasis on methods used in our laboratory. This will be followed by results on a number of metals studied in our group at Chicago, and finally by an attempt to rationalize these results. The metallicity of ultrathin metal layers has also been addressed by Plummer, Dowben and co-workers,^{3–5} with emphasis on alkali and alkaline earth metals, as well as Hg. The present work looks at Cu,⁶ Ag,^{7,8} Ni,^{9,10} Pd,^{11,12} and Hg.¹³

What Is a Metal?

When a large number of atoms coalesce into a solid, there is overlap of orbitals, leading to bonding and antibonding combinations, and corresponding energy levels, just as in "ordinary" molecules. Since the number of interacting atoms in a solid is $\sim 10^{23}$, the spacing between individual energy levels becomes extremely small and the original atomic levels broaden into bands of quasi-continuous energy. Energies lying outside these bands are forbidden. The width of bands depends on the overlap of the atomic orbitals from which they were formed, so that low-lying levels form narrower bands than higher ones. In many cases the broadening is insufficient to lead to overlap of different bands although this can happen and in fact accounts for the metallicity of alkaline earth metals. In insulators and semiconductors bonding and antibonding bands do not overlap but are separated by an energy

gap. In metals a single band containing N states will show both bonding (strongest near the bottom) and antibonding (most pronounced near the top) character. Electrons can occupy the individual, closely spaced orbitals within a band at most pairwise, allowing for spin, so that levels in each band will be filled until all electrons in that band have been accommodated. In a metal, the highest occupied band is only partially filled. For example, in Na the 3s band contains N states, but since each atom contributes only one electron, the band will be half-filled.

The highest filled level, the Fermi level, has an energy E_F several electronvolts, i.e., $\sim 10^4$ K, above the bottom of the conduction band, so that the electron distribution at room temperature differs only very slightly from that at 0 K. E_F also corresponds to the chemical potential of electrons in the metal and lies several electronvolts below the vacuum level, i.e., the lowest potential energy of an electron outside the metal. This energy difference is known as the work function, here called ϕ . Since different planes of the same metal have different atomic arrangements which lead to differences in electron density contours and hence surface dipole moments, different planes show different ϕ , with atomically open, i.e., "rough", planes having the lowest values.

Although thermal excitations above E_F contribute only a small "Boltzmann tail" to the electron distribution at moderate temperatures, the existence of empty states just above the Fermi level gives a metal its characteristic properties, namely, high electrical conductivity, the ability to screen out the potential produced by external or internal charges in distances of ~ 0.5 Å, and the ability to sustain collective electron (so-called plasma) oscillations. This can be seen very easily in a qualitative way: If a moderate electric field is applied to a solid, a force is exerted on electrons, but these can move only if there are empty states into which they can be excited. Screening requires redistribution of mobile charge in response to an applied potential, and this also requires available empty states. To a first approximation a potential is attenuated by a factor of $e^{-k_s r}$ where the screening length $1/k_s$ is defined by

- (1) Campbell, C. T. *Annu. Rev. Phys. Chem.* **1990**, *41*, 775.
- (2) Rodriguez, J. P.; Goodman, D. W. *J. Phys. Chem.* **1991**, *95*, 4196.
- (3) Plummer, E. W.; Dowben, P. A. *Prog. Surf. Sci.* **1993**, *42*, 201.
- (4) Plummer, E. W.; Carpinelli, J. M.; Weitering, H. H.; Dowben, P. A. *Phys. Low-Dimens. Struct.* **1994**, *4/5*, 99.
- (5) Dowben, P. A.; McIlroy, D. M.; Zhang, J.; Rühl, E. *Mater. Sci. Eng.*, *B.*, in press.
- (6) Shamir, N.; Lin, J. C.; Gomer, R. *J. Chem. Phys.* **1989**, *90*, 5135.
- (7) Zhao, Y. B.; Gomer, R. *Surf. Sci.* **1993**, *280*, 125.
- (8) Zhao, Y. B.; Gomer, R. *Surf. Sci.* **1993**, *280*, 138.
- (9) Whitten, J. E.; Gomer, R. *Surf. Sci.* **1994**, *316*, 36.
- (10) Whitten, J. E.; Gomer, R. *J. Phys. Chem.* **1995**, *99*, 2826.
- (11) Lin, J. C.; Shamir, N.; Gomer, R. *Surf. Sci.* **1990**, *226*, 26.
- (12) Zhao, Y. B.; Gomer, R. *Surf. Sci.* **1992**, *273*, 285.
- (13) Zhao, Y. B.; Gomer, R. *Surf. Sci.* **1992**, *271*, 85.

Robert Gomer is the Carl William Eisendrath Distinguished Service Professor in the Department of Chemistry and the James Franck Institute of the University of Chicago. He was born in Vienna, Austria, and received a B.A. from Pomona College in 1944. Following a stint in the U.S. Army, he received a Ph.D. from the University of Rochester in 1949. After a year as research associate at Harvard, he joined the University of Chicago in 1950. His research interests include chemisorption and diffusion on metal surfaces. He is a member of the National Academy of Science, the American Academy of Arts and Sciences, and the Leopoldina Akademie. He is the recipient of the Kendall and Adamson awards of the American Chemical Society, the Davison-Germer Prize of the American Physical Society, and the Welch award of the American Vacuum Society.

$$k_s^2 = 4\pi e^2 \rho(E_F) \quad (1)$$

where e is electron charge and $\rho(E_F)$ is the density of states per unit volume at the Fermi level, i.e., $(dN/dE)_{E_F}$, N being the number of states per unit volume. Equation 1 is generally derived in elementary discussions for a free electron gas,¹⁴ for which k_s depends only very weakly on electron density n_0 ; namely, $k_s \propto n_0^{1/6}$. However, eq 1 is more generally valid, as shown for instance by Ehrenreich and Cohen.¹⁵

Plasma oscillations correspond to the sloshing back and forth of the entire mobile electron population, with ion cores providing the restoring force, i.e., constitute a longitudinal long wavelength displacement, which can be excited by electrons impinging on a metal. They are predicted by Maxwell's equations when the real part of the frequency dependent dielectric constant ϵ is 0 and have angular frequency ω_p .^{14,16}

$$\omega_p = [4\pi n_0 e^2 / m(1 - \delta\epsilon)]^{1/2} \quad (2)$$

where n_0 , e , and m are electron density, charge, and mass, respectively, and $\delta\epsilon$ is a correction to the free electron form of ϵ , taking intra- and interband transitions into account. In addition to bulk plasmons which can be excited in any direction, including that parallel to the surface, there also exists a surface plasmon, which can only correspond to an oscillation parallel to the surface. Its existence requires that the sum of the dielectric constants inside and outside the metal be zero, so that

$$\omega_s = \omega_p [(1 - \delta\epsilon)/(2 - \delta\epsilon)]^{1/2} \approx \omega_p / 2^{1/2} \quad (3)$$

For most metals $\hbar\omega_p \approx 10$ eV; i.e., $\nu_p \approx 10^{16}$ s⁻¹.

Most properties of solids depend on their translational symmetry. Among these are of course diffraction effects including the details of the momentum (i.e., k) dependence of band structures. dc conductivity also depends on periodicity and is severely degraded in some disordered solid metals, because of some electron localization in regions of favorable potential energy. (In liquid metals ion core positions are not frozen in but subject to thermal fluctuation so that considerable electron mobility and hence conductivity results.) However, screening and plasma excitations do *not* depend strongly on long-range order in many cases. The reason is clear: the number of orbitals and the number of electrons do not depend on order; the bands themselves result from combinations of atomic orbitals, which will occur even in disordered metals, so that there will be a finite density of states at E_F . While plasma oscillations have long wavelengths, individual electron displacements are quite small. Roughly they are given by $v_F/2\nu_p$. The Fermi velocity $v_F \approx 10^8$ cm/s¹⁴ (i.e., the velocity of electrons at the Fermi level) while we have seen that $\nu_p \approx 10^{16}$ s⁻¹. Thus, the displacement of an electron is on the order of atomic dimensions and insensitive to disorder.

Loss of Metallicity

We next consider what might destroy metallicity, particularly in ultrathin layers. First, at low densi-

ties, i.e., large interatomic spacing, there can be a Mott metal-insulator transition.¹⁷ In the simplest one-electron picture a conduction band would simply get narrower and narrower as interatomic spacing increased and overlap decreased. However, the concomitant reduction in electron density leads to increases in screening length and thus to less screening of ion core potentials. At a certain critical electron concentration the latter becomes sufficiently unscreened to create bound states on individual ion cores, i.e., to formation of an insulator. Apparently this happens in Cs monolayers below their close-packed density³ because of the large Cs diameter. Metal-insulator transitions are also affected by the Coulomb repulsion U of two electrons "sitting" on the same ion core. If U is large, it will also drive localization of single electrons on ion cores. U is also affected by screening.

Second, a Peierls distortion¹⁴ can occur. This corresponds to a restructuring of a lattice in such a way as to introduce a new periodicity and a band gap at E_F . Levels below the gap will then be filled, levels above it empty. Since the new full band has lower energies near its top than before the splitting, a net lowering of energy results. While Peierls distortions can occur in two dimensions, this need not lead to insulator formation as in one dimension, i.e., for chains of atoms.

Third, the width of a band is proportional to the number of nearest neighbor interactions, as well as to their strengths. Thus, for a simple cubic lattice the band width in two dimensions is reduced from 12γ to 8γ in the so-called tight binding approximation in which γ represents the hopping matrix element between neighbors. This reduction carries over into more sophisticated calculations. γ itself decreases rapidly with increasing spacing. Thus, it may happen that bands which overlap in three dimensions, e.g., 6s and 6p in Hg or 3d and 4s in Ni, no longer do so in two dimensions. The consequences would be a full 6s band in the former and a full 3d band in the latter case with empty 6p and 4s bands, respectively, and consequent loss of metallicity. The effect of the number of nearest neighbors on metallicity was already considered by Miedema and Dorleijn.¹⁸

Metallicity is not an absolute. There can be intermediate situations, since there can be *some* $\rho(E_F)$ and hence *some* screening even when a layer is not fully metallic and there can be plasma oscillations which take electrons across gaps of energy $< \hbar\omega_p$.

Preparation of Metal Monolayers

Since it is impossible to prepare free-standing monolayers, many experiments have been carried out by deposition on metal or semiconductor surfaces which makes it possible to attain a high degree of order by suitable annealing. The main disadvantage of direct deposition is the possibility of strong interaction between the substrate and the overlayer, which can modify its electronic properties substantially. We have taken a slightly different approach, namely, deposition of the metal M to be studied on a close-packed tungsten surface, precovered with a chemi-

(14) Kittel, C. *Introduction to Solid State Physics*, 6th ed.; J. Wiley & Sons: New York, 1988.

(15) Ehrenreich, H.; Cohen, M. H. *Phys. Rev.* **1959**, *115*, 786. Wiser, N. *Phys. Rev.* **1963**, *129*, 62.

(16) Raether, H. *Springer Tracts Mod. Phys.* **1965**, *38*, 93.

(17) Mott, N. F. *Proc. R. Soc. London* **1982**, *A382*, 1; *Metal-Insulator Transitions*; Taylor & Francis: London, 1990.

(18) Miedema, A. R.; Dorleijn, J. W. F. *Philos. Mag.* **1981**, *B43*, 251.

sorbed spacer layer, i.e., formation of M/S/W(110) sandwiches, S standing for spacer. The latter were H, O, CO, and chemisorbed benzene. CO is adsorbed on W via the C end; benzene is adsorbed flat.¹⁰ Both form more or less close-packed layers, whose densities are determined by their respective van der Waals dimensions. The coverage of CO on a W(110) surface¹⁹ is $\sim 10^{15}$ molecules cm^{-2} , so that an overlayer of M can be supported on top of CO, with some M atoms directly on top of O and others wedged between CO molecules but still separated from the W surface. The density of benzene on the surface is¹⁰ $\sim 2 \times 10^{14}$ molecules cm^{-2} , corresponding to a van der Waals diameter ~ 7 Å. Thus, M atoms will "sit" either on top of the benzene ring or on top of H atoms between the rings. Consequently CO and benzene provide physical separation between M and the W surface, which is not the case for H or O. However, the latter passivate the W surface so that interaction with W is largely avoided. There may of course be some chemical interaction with the spacer itself, particularly O, although the latter interacts primarily with W. For CO this is probably a very minor effect. Unfortunately Ni and Pd displace (but do not desorb) CO^{9,11} so that physical separation here requires benzene as the spacer. A disadvantage of the spacer method is the impossibility of annealing the composite layer without dewetting of the overlayer metal. Thus, the formation and maintenance of M/S/W(110) structures requires deposition and measurements at $T \approx 90$ K. Most M layers will therefore not be fully ordered, and some piling up into second or higher layers can occur below nominal monolayer coverages. LEED indicates that ordered M monolayers are formed only on H/W(110). Piling up, but not degree of ordering or monolayer island formation, can be monitored by following the intensity of Auger lines of M, S, and W as a function of M coverage. This will be illustrated presently.

Experimentally Accessible Criteria of Metallicity

We restate first what we are looking for, namely, extended states, i.e., delocalized electrons, with a finite density of states at and above E_F , from which follow electrical conductivity, screening, and plasma oscillations. To date direct conductivity measurements have not been done and seem more or less impossible for direct deposition on metal or semiconductor substrates, as well as for M/S/W sandwiches. Densities of states at and below E_F can be obtained by photoemission and above E_F by inverse photoemission. (In the latter case, electrons of known energy are allowed to fall into empty states and the frequency of emitted radiation is measured.) However, these measurements cannot easily distinguish between localized and extended states, although angle-resolved photoemission can probe band structure, if there is no interference from the substrate bands.

Screening can be investigated in various ways. Dowben and co-workers²⁰ have looked for changes in core hole screening in resonant photoemission. Resonant photoemission is a very complex phenomenon, and interpretation is not always straightforward. We

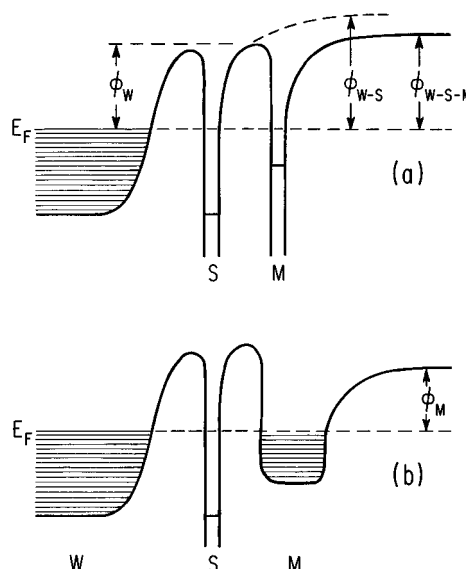


Figure 1. Schematic diagram illustrating M/S/W potentials for M/S/W sandwiches (a) without metallicity of M and (b) with M forming a metallic layer. The subscripts on ϕ indicate the relevant dipole layer potential contributions to the work function. In (b) the thickness of the M layer has been exaggerated. Horizontal lines indicate energy levels.

use a different approach, namely, to measure the work function ϕ of M/S/W(110) sandwiches, which also shows how closely it approaches that of bulk M. The rationale is illustrated in Figure 1. If individual M atoms interact with the S/W(110) surface by forming bonds or van der Waals complexes, with associated dipole moments, the work function will be that of W(110) plus the potentials of the W–S and S–M dipole layers (Figure 1a). On the other hand if the M layer is metallic and has a set of band states, filled to the Fermi level, the W–S and S–M potentials (there can of course still be some S–M interaction) will be screened out. M and W must have a common Fermi level, i.e., chemical potential of electrons, which can easily be accomplished by a small amount of electron transfer via tunneling through S. Thus, the measured ϕ will be that of the metallic M layer, as shown in Figure 1b. Even if there is perfect screening, it is still not obvious how this work function relates to that of bulk M, and this question is interesting *per se*. For a given spacer S there is always the possibility that the sum of dipoles could give a ϕ value similar to that of M. This can be excluded if ϕ is nearly independent of S or its coverage.

Collective excitations can be examined by electron energy loss measurements: A beam of fairly monochromatic electrons is allowed to impinge on the M/S/W(110) (or M/W) surface and the energy spectrum of reflected electrons examined in the vicinity of the elastic peak.

Experimental Details

The apparatus and procedures used in our work have been described in some detail previously.^{21,22} Experiments are carried out in an ultrahigh vacuum apparatus (Figure 2) using standard techniques of surface science including the use of a vibrating electrode (Kelvin probe) for work function measure-

(19) Wang, C.; Gomer, R. *Surf. Sci.* **1978**, *74*, 389.

(20) Dowben, P. A.; LaGraffe, D.; Li, D.; Vidali, G.; Zhang, L. *Phys. Rev.* **1991**, *B43*, 10677.

(21) Steinbrüchel, Ch.; Gomer, R. *Surf. Sci.* **1977**, *67*, 21.

(22) Opila, R.; Gomer, R. *Surf. Sci.* **1983**, *127*, 569.

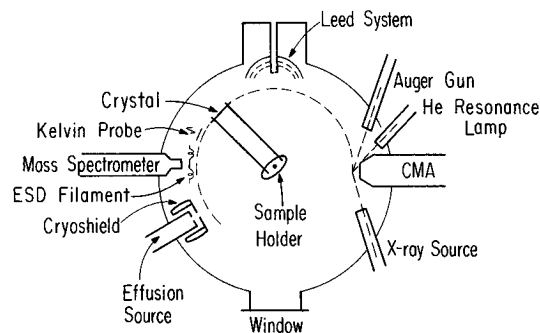


Figure 2. Schematic diagram of the experimental apparatus. The metal evaporation source (not shown for simplicity) is located between the LEED system and the CMA in the plane of the crystal. The Auger gun, He resonance lamp, and X-ray source shine down onto the crystal from above. CMA stands for cylindrical mirror and analyzer and is an electrostatic device for measuring the kinetic energies of UV or X-ray photoelectrons, Auger electrons, or quasi-elastically reflected electrons for loss measurements.

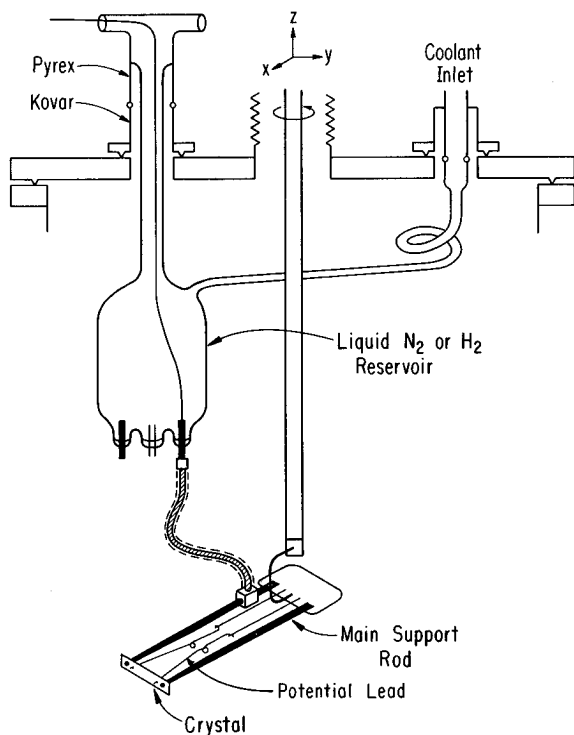


Figure 3. Schematic diagram illustrating the cooling and heating arrangement for the rotatable crystal. Only one of the main Cu braids and neither of the potential lead connections are shown. For cooling, the bulb is filled with liquid coolant and the braids serve to cool the crystal. For heating, a dc current is passed via the braids through the crystal and the resistance of the latter determined from this current and the voltage between the potential leads. The crystal temperature is a known function of its resistance. A temperature controller can either maintain the crystal at the desired T or ramp the temperature continuously at a preset rate for desorption measurements.

ments.²³ The substrate is a thin slab of (110) oriented tungsten which can be positioned in front of the various devices in the system. It can be cooled to 27 K via liquid H_2 or 90 K via liquid N_2 contained in a bulb to which the crystal is connected via flexible Cu braids (Figure 3). It can also be heated resistively to the desired T or flashed to 2700 K for cleaning.

Since work function measurements are central to this work, a very brief description of the Kelvin

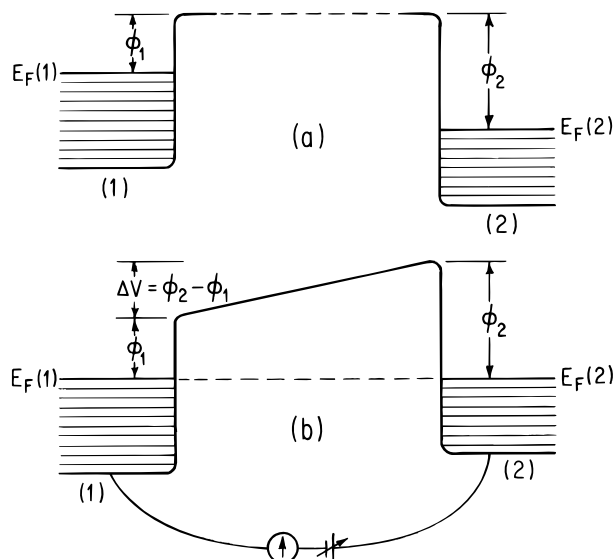


Figure 4. Schematic potential energy diagrams (as seen by electrons) illustrating the Kelvin method of determining work function differences: (a) metals 1 and 2 isolated from each other (the vacuum levels line up); (b) after connection via a wire, with no voltage on the battery (the Fermi levels now line up, and the vacuum levels differ by the contact potential $\Delta V = \phi_2 - \phi_1$). If the spacing between metals 1 and 2 is varied at some frequency f , changing the capacitance between metals 1 and 2, an alternating current will flow through the wire. Equality of the vacuum levels is restored if the battery makes metal 1 more negative than metal 2 by ΔV , and at this point zero current flows through the wire.

method is given here. Consider two different metals with work functions ϕ_1 and ϕ_2 facing each other (Figure 4a). In the absence of stray charges, there is no potential difference between them and the vacuum levels line up. Now connect these metals by a wire, so that charge can flow. Since the Fermi levels correspond to the chemical potentials of electrons, these must become equal, and this is accomplished by electrons flowing through the wire from metal 1 to metal 2 until the Fermi levels are equal. This does *not* require a substantial flow. Rather, the small amount q of electron charge transferred piles up on the surface of metal 2, with a corresponding deficit on metal 1, thereby raising the potential of metal 2 relative to metal 1, and establishing a potential difference (known as the contact potential), $\Delta V = \phi_2 - \phi_1$. Thus, the two surfaces constitute a capacitor of fixed ΔV (Figure 4b). However, the charge required to maintain ΔV depends on the capacitance C , and the latter depends on the spacing of the two surfaces. If this is changed, charge will flow through the wire to maintain the relation $C\Delta V = q$. If one of the surfaces, the reference electrode, say metal 2, is vibrated at fixed frequency, an alternating current will flow through the wire and can be measured by a suitable "ammeter". Now add a variable battery to the circuit. When its voltage just balances ΔV , the potential difference between metals 1 and 2 is zero and no current flows when C is varied. If the reference electrode is inert and shielded from metal adsorption, so that ϕ_2 is constant, ϕ_1 can be found if ϕ_2 is known. In practice the current through the circuit is converted to a voltage, and this is fed into a lock-in amplifier driven in phase by an oscillator which also drives a solenoid which vibrates the reference electrode, and

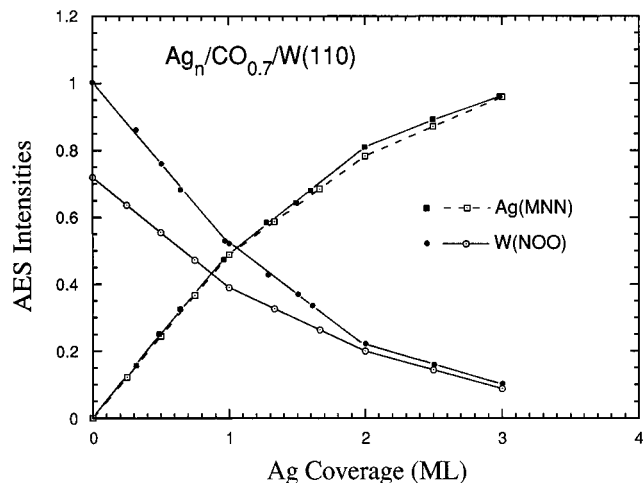


Figure 5. Ag(MNN) and W(NOO) Auger intensities vs Ag coverage in monolayers on clean and CO-covered W(110). The solid points correspond to clean and the open ones to CO-covered W(110). In the latter case the W(NOO) intensity is diminished by CO. The data are from ref 7.

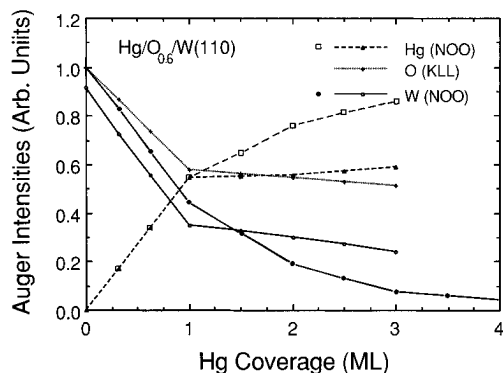


Figure 6. Auger intensities of the Hg(NOO), O(KLL), and W(NOO) Auger lines vs Hg deposition in monolayers for clean W(110) (\square) and O-covered W(110) (\triangle and \circ). Note the marked decreases in slope of all lines beyond $n = 1$ in the latter case. The data are from ref 13.

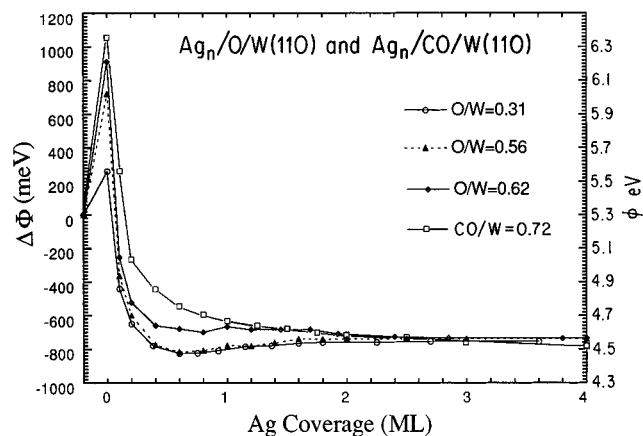


Figure 7. Work function increment $\Delta\phi$ relative to clean W(110) and absolute work function ϕ vs Ag coverage in monolayers for various O and one CO coverage on W(110). Note the different initial ϕ values before Ag adsorption and the near equality of all curves for $n > 1$. The data are from ref 8.

the circuit is operated as a feedback loop which automatically balances itself and allows ΔV to be read or fed to a computer. The method is generally used to measure differences in ϕ_1 , for instance, by first measuring ΔV corresponding to the clean surface of metal 1 and then again after adsorption, and so on.

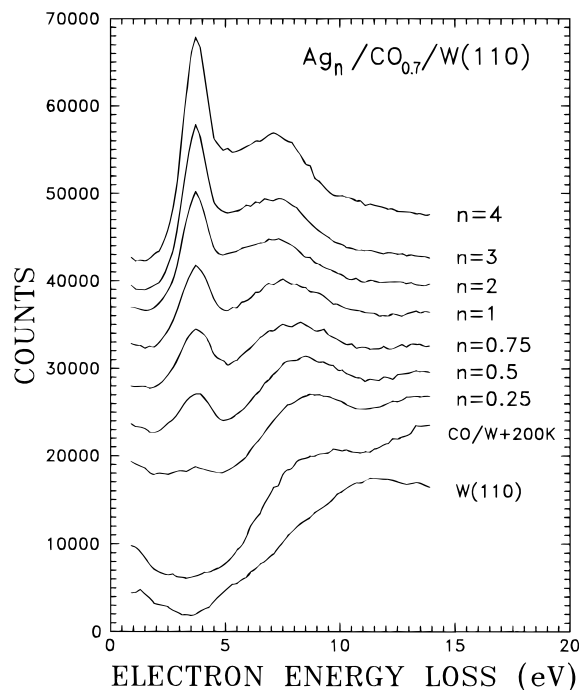


Figure 8. Energy loss peaks for various Ag coverages on CO/W(110). Reprinted with permission from ref 8. Copyright 1993 Elsevier Science.

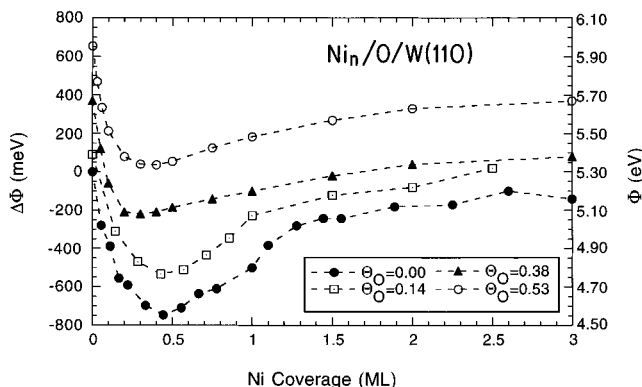


Figure 9. Work function increments $\Delta\phi$ relative to clean W(110) and absolute work function ϕ vs Ni coverage in monolayers for various initial O coverages. θ corresponds to O/W. Reprinted with permission from ref 9. Copyright 1994 Elsevier Science.

Some Results

Figures 5–9 show some representative results. A summary of work function and electron excitation, i.e., loss peak results, is given in Table 1. Figure 5 shows Auger results for Ag on clean W(110) and on $\text{CO}_{0.7}/\text{W}(110)$.⁷ The subscript here refers to the CO/W ratio, which corresponds to near saturation for CO. The curves are nearly identical, rise linearly to the monolayer point, and then show reduced slope for each subsequent layer with distinct breaks at monolayer completion points. These result from attenuation of emission from the first layer by the second one, and so on. Thus, growth is layer by layer even on CO. By contrast Figure 6 shows comparable data for Hg¹³ on clean and oxygen-covered W(110) at 90 K. On clean W(110) growth is layer by layer at 90 K. On O/W(110) the Hg(NOO) intensity rises linearly to the first monolayer point, but then nearly levels off. Concomitantly the O(KLL) and W(NOO) intensities also nearly level off. This indicates that growth is good to $n = 1$,

Table 1. Summary of Work Functions and Loss Energies

surface	ϕ , eV	loss energies, eV	remarks
W(110)	5.30	12, 21.5	
O _{0.5} /W(110)	6.00		
H ₁ /W(110)	4.80	21	
Bz ₁ /W(110)	3.78		
CO _{0.7} /W(110)	6.40	9.55, 14	
Cu(111)	4.94		
Cu(poly)	4.65	7.6 ^{15,24}	
Cu ₂ /W(110)	4.58	9.0	at $n = 8$, losses at 4.64 and 7.6 eV
Cu ₁ /O _{0.85} /W(110)	5.18	not measured	
Cu ₂ /O _{0.85} /W(110)	4.92	not measured	
Cu ₁ /O _{0.62} /W(110)	4.76	4.64, 12	4.64 eV loss seen for $n \geq 0.2$
Cu ₂ /O _{0.62} /W(110)	4.78	not measured	
Cu ₁ /O _{0.30} /W(110)	4.65	not measured	
Cu ₁ /CO _{0.7} /W(110)	4.65	4.64, 9.0	losses seen for $n \geq 0.4$
Cu ₂ /CO _{0.7} /W(110)	4.57	4.64, 8.0	
Ag(111)	4.74		
Ag(poly)	4–4.3	4.0, ¹⁵ 7.0 ¹⁵	
Ag ₃ /W(110)	4.57	4.9, 7.8	losses only for $n \geq 2$
Ag ₁ /O _{0.62} /W(110)	4.63	3.7, 7.8	losses seen for $n \geq 0.5$
Ag ₃ /O _{0.62} /W(110)	4.56	3.7, 7.8	
Ag ₁ /O _{0.31} /W(110)	4.50	not measured	
Ag ₃ /O _{0.31} /W(110)	4.56	not measured	
Ag ₁ /CO _{0.7} /W(110)	4.67	3.5, 7.5	losses seen for $n \geq 0.5$
Ag ₃ /CO _{0.7} /W(110)	4.51	3.5, 7.5	
Ag ₁ /H ₁ /W(110)	4.55	4.5, 8	
Ag ₃ /H ₁ /W(110)	4.51	3.9, 8	
Ag ₁ /Bz ₁ /W(110)	3.94	4.0, 7.8	
Ag ₃ /Bz ₁ /W(110)	4.30	4.0, 7.8	
Hg(poly)	~4.5	6.4 ²⁷	
Hg ₁ /W(110)	5.08		plasmon for $n = 2$ at ~8.0 eV for $n = 4$, $\phi = 4.55$ eV
Hg ₅ /W(110)	4.65	7.0	
Hg ₁ /O _{0.3} /W(110)	4.85	not measured	
Hg ₁ /O _{0.57} /W(110)	4.68	not measured	
Hg ₁ /O _{0.66} /W(110)	4.66	8.5 (weak)	
Hg ₁ /H ₁ /W(110)	4.63	7.0	
Hg ₃ /H ₁ /W(110)	4.65	7.0	
Hg ₁ /CO _{0.7} /W(110)	5.60	8	
Hg ₅ /CO _{0.7} /W(110)	5.05	6.8	loss for $n \geq 1.5$
Pd(111)	5.55		
Pd(poly)	5.22	7.5 ²⁹	
Pd ₁ /W(110)	4.90	10	$\phi(\text{min}) = 4.68$ eV at $n = 0.5$
Pd ₂ /W(110)	5.46	9	loss shifts to 8 eV for $n = 8$
Pd ₁ /O _{0.27} /W(110)	5.40	not measured	$\phi(\text{min}) = 5.35$ eV at $n = 0.4$
Pd ₂ /O _{0.27} /W(110)	5.40		
Pd ₁ /O _{0.47} /W(110)	5.34		$\phi(\text{min}) = 5.00$ eV at $n = 0.35$
Pd ₂ /O _{0.47} /W(110)	5.50		
Pd ₁ /O _{0.62} /W(110)	5.18	9 (weak)	$\phi(\text{min}) = 4.82$ eV at $n = 0.4$
Pd ₂ /O _{0.62} /W(110)	5.52	9	
Pd ₁ /H ₁ /W(110)	5.18	8.5	
Pd ₃ /H ₁ /W(110)	5.44	8.5	
Ni(111)	5.42	8.1 ³⁰	
Ni(poly)	5.15		
Ni ₁ /W(110)	4.80	9.5	$\phi(\text{min}) = 4.55$ eV at $n = 0.45$
Ni ₃ /W(110)	5.15	8.5	
Ni ₁ /O _{0.14} /W(110)	5.05	not measured	$\phi(\text{min}) = 4.75$ eV at $n = 0.45$
Ni _{2.5} /O _{0.14} /W(110)	5.32	not measured	
Ni ₁ /O _{0.38} /W(110)	5.23	not measured	$\phi(\text{min}) = 5.07$ eV at $n = 0.3$
Ni ₃ /O _{0.38} /W(110)	5.37	not measured	
Ni ₁ /O _{0.53} /W(110)	5.50		$\phi(\text{min}) = 5.35$ at $n = 0.35$
Ni ₃ /O _{0.53} /W(110)	5.68		
Ni ₁ /H ₁ /W(110)	5.30		$\phi(\text{min}) = 4.75$ at $n = 0.1$
Ni ₃ /H ₁ /W(110)	5.30		
Ni ₁ /Bz ₁ /W(110)	4.08		
Ni ₃ /Bz ₁ /W(110)	4.28		

after which piling up into Hg clusters occurs. Most systems studied are intermediate between Ag and Hg, showing linear increases and breaks at monolayer points but generally with somewhat reduced slopes relative to deposition on clean W. This corresponds either to minor piling up or to the effect of the spacer S on the transition probabilities of Auger processes in M atoms. Figure 7 shows ϕ vs Ag coverage on various O coverages and for CO on W(110).⁸ For $n = 1$ the ϕ values are 4.5 eV for the two lower O coverages and 4.6 eV for the highest O coverage and for CO. This

indicates slightly less screening in the latter two cases where $\Delta\phi$ before Ag adsorption is ~1 eV. For $n \geq 1$ all ϕ values converge to 4.51–4.55 eV, very close to that of Ag multilayers on W(110) and intermediate between those of Ag(111) and polycrystalline Ag, as indicated in Table 1. Figure 8 shows energy loss spectra for Ag_n/CO/W(110).⁸ These show a 3.6 eV loss and a second loss peak shifting from 8 to 7 eV with increasing Ag coverage. The former is probably a surface plasmon, but has also been interpreted as an interband transition.¹⁶ The latter corresponds to a

bulk plasmon.¹⁶ It is interesting that these loss features already appear at submonolayer coverages. This could correspond to formation of patches of close-packed Ag, although this would require high mobility of Ag on top of CO. Since the mean Ag–Ag separations are on the order of 2.7 Å at $n = 1$ and only increase to 5.6 Å at $n = 0.25$, it is also conceivable that Ag plasmons occur for local $n < 1$, although in this case one would expect a shift with coverage. In any case plasmons clearly exist. Figure 9 shows ϕ vs Ni dose for various O coverages on W(110).⁹ The values at $n = 1$ vary widely and do not merge even at $n = 3$, varying by more than 350 meV from low to high O coverage. No plasmons were seen.

We turn next to the results shown in Table 1. The table lists relevant ϕ values and loss energies (where known) for W(110), for $S_x/W(110)$, and for $M_n/S_x/W(110)$. Here n stands for the number of monolayers of M, with $n = 1$ not necessarily corresponding to an M/W atom ratio of unity. x stands for S coverage in units of S/W, with $x = 1$ corresponding to 1.42×10^{15} S/cm². The exception is benzene, where $Bz_1/W(110)$ refers to a saturated monolayer of chemisorbed Bz containing¹⁰ $\sim 2 \times 10^{14}$ molecules cm⁻². Data for the highest and lowest work function planes of bulk M are also shown.²⁴

For Cu⁶ on various O/W(110) layers and on CO_{0.7}/W(110) ϕ is close to that for polycrystalline Cu at $n = 1$, with the exception of the O/W = 0.85 layer, prepared by dosing Cu₁/O_{0.6}/W(110) with additional O₂ and heating to high temperature to desorb Cu.²⁵ This layer may be structurally different from the other ones. There is an energy loss near 4 eV, which was originally interpreted by us⁶ as an interband transition, since it appears at submonolayer coverages without a shift in energy as Cu coverage increases. It has also been seen on bulk Cu surfaces and similarly interpreted,²⁵ but could also be a surface plasmon. For Cu/CO_{0.7}/W(110) there is also a loss at 8–9 eV and for Cu/O/W(110) at 12 eV. These may correspond to a shifted bulk plasmon.^{10,26} High-resolution electron energy loss measurements by Houston et al.²⁷ show that the C–O stretch and the W–O stretch for CO/W(110) and O/W(110) are severely attenuated by a monolayer of Cu on top of these. This is just what one would expect if the latter is metallic, forming images of the W–O and C–O dipoles, converting them to quadrupoles, and thus reducing their oscillator strengths. Comparable attenuation of the IR absorption of the C–O stretch in Cu/CO/Ru(100) was seen by Hoffman et al.²⁸ We thus conclude that Cu monolayers meet our criteria of metallicity.

Many results for Ag have already been discussed. Adsorption on Bz₁/W(110),¹⁰ where ϕ must increase, rather than decrease, to reach the Ag value does so but only to 3.94 eV for $n = 1$ and 4.3 eV for $n = 3$. This is still in the range for polycrystalline Ag. The losses seen on other spacers also occur on Bz₁/W(110). Thus, Ag monolayers are metallic on all substrates used.

Hg layers have been examined by Dowben and co-workers^{3–5} who conclude that one monolayer on W(110) behaves metallically. Our results¹³ indicate that ϕ for Hg₁/W(110) is still far from that of bulk Hg and does not reach the latter until $n \geq 5$. We see only a very weak plasmon at $n = 1.5$, which develops strength and shifts slightly with increasing Hg thickness. However, on O/W(110) and H/W(110) ϕ approaches the bulk Hg value at $n = 1$, and shows on the former a shifted and on the latter a normal surface plasmon²⁹ at 7 eV. Since Hg seems to pile up on O/W(110) after the first Hg layer, we ignore ϕ values beyond this coverage. Incidentally the results on H/W(110) suggest that H decouples the W surface electronically from Hg, although the latter is still in physical contact with W. The situation is more complex on CO/W(110). Here the work function results indicate very imperfect screening even for relatively thick Hg deposits. Nevertheless, there is a surface plasmon loss at 8 eV for $n = 1$ which shifts to 6.8 eV for $n \geq 1.5$ and increases in intensity with increasing n . This argues against Hg pileup for $n > 1$. Calculations by Freeman and co-workers³⁰ indicate that the metallicity of Hg monolayers depends sensitively on Hg–Hg spacing. This is apparently sufficiently small on O- and H-covered W(110) but too large on CO/W(110). Since plasmon energies are high, they can still be excited even though the Hg layer on CO does not screen. Thus, Hg is not uniformly metallic.

Pd on O/W(110)¹¹ shows ϕ minima at submonolayer coverages, suggesting O–Pd dipole formation with some coverage dependent self-depolarization. At $n = 1$, ϕ values vary slightly with O coverage, but approach that of Pd(111) at $n = 2$. On H/W(110)¹² ϕ is less than that of Pd(111) at $n = 1$ but approaches it at $n = 3$. There are plasmons on O/W(110) and H/W(110) close to the bulk value, 7.5 eV.³¹ Thus, Pd shows some screening and approaches metallic behavior for $n \geq 2$.

Work function results for Ni on O/W(110)⁹ are shown in Figure 9. These depend strongly on O coverage at $n = 1$ and still differ by >300 meV at $n = 3$ but then lie between that for Ni(111) and polycrystalline Ni. For Ni on H/W(110)⁹ $\phi = 5.30$ for $n \geq 1$; i.e., ϕ is between the values for Ni(111) and polycrystalline Ni, but 380 meV less than the value for Ni₃/O_{0.53}/W(110). On Bz₁/W(110)¹⁰ ϕ is only 4.28 eV for $n = 3$. There are no observable plasmons on any of these surfaces, although losses occur on Ni₁/W(110)⁹ and Ni₃/W(110)⁹ at 9.5 and 8.5 eV, respectively, corresponding to a Ni surface plasmon.³² Thus, Ni screens poorly and shows no collective excitations on O, H, or Bz spacers.

For systems showing metallicity, plasmons appear and ϕ values approach those of bulk M at much lower coverages than on clean W(110), indicating substantial physical and/or electronic decoupling by spacers.

(24) Hölzl, J.; Schulte, F. K. *Springer Tracts Mod. Phys.* **1979**, *85*, 1.

(25) Lin, J. C.; Shamir, N.; Gomer, R. *Surf. Sci.* **1988**, *206*, 86.

(26) Robins, J. L.; Swan, J. B. *Proc. Phys. Soc., London* **1960**, *76*, 857.

(27) Houston, J. E.; O'Neill, D. G.; Gomer, R. *Surf. Sci.* **1991**, *244*, 221.

(28) Hoffman, F. M.; Rocker, G.; Tochiyama, T.; Martin, M.; Metiu, H. *Surf. Sci.* **1988**, *205*, 397.

(29) Kim, B. O.; Lee, G.; Plummer, E. W.; Dowben, P. A.; Liebsch, A. *Phys. Rev.* **1995**, *B52*, 6057.

(30) Hansen, H. J. F.; Freeman, A. J.; Weinert, M.; Wimmer, E. *Phys. Rev.* **1983**, *B28*, 593.

(31) Nishijima, N.; Yo, M.; Kuwahara, Y.; Onchi, M. *Solid State Commun.* **1986**, *58*, 75.

(32) Heimann, B.; Hölzl, J. *Phys. Rev. Lett.* **1971**, *26*, 173.

Interpretations

How can these results be understood? The answer for Cu and Ag is straightforward. These metals have filled d and half-filled s bands. Thus, given sufficient overlap and electron density to prevent them from being Mott insulators, they must necessarily show some metallicity. The metallicity of Hg layers depends on overlap of 6s and 6p bands, which seems very sensitive to Hg–Hg spacing,³⁰ as already pointed out. Thus, it is not surprising that metallicity depends more sensitively on the details of layer structure than for Cu and Ag.

For Pd and Ni with formal structures $4d^95s^1$ and $3d^94s^1$, the reduced strengths and numbers of hopping matrix elements in very thin layers could narrow the s bands to the point where overlap with the d bands is reduced, the latter becoming nearly full and the former nearly empty, with a resultant decrease in or loss of metallicity. However, Burdett and co-workers^{33,34} calculate that an isolated close-packed Ni monolayer should be metallic but that interaction with either O or Bz on W(110) destroys this. The argument for O is as follows: Interaction of O with Ni leads to formation of a bonding orbital with largely O 2p character and an antibonding one with largely Ni 4s character. Since it is antibonding, the latter is pushed up in energy, no longer overlaps with the 3d band, and thus is empty. Similar results were calculated for Ni on Bz₁/W(110). Although O and Bz interact very strongly with underlying W, O on W still affects what

is above it. For instance, hydrogen adsorption is reduced even on Ni₃/O_{0.5}/W(110) relative to Ni₃/W(110).³⁵ Thus, O interaction with Ni may be sufficiently strong to make the Burdett model applicable.

What is in a way more surprising and certainly not fully understood is that ϕ and plasmon energies for mono- or at most bilayers can come close to bulk values, i.e., three-dimensional values, for Cu, Ag, and Hg (except on CO).³⁶

Concluding Remarks

This Account has presented some observations on ultrathin layers, which strongly suggest that Ag, Cu, and Hg monolayers are metallic with Pd less metallic and Ni almost wholly nonmetallic. One of the weaknesses of this work is the absence of detailed structural information (except on H/W(110)), which could be obtained via ultrahigh-vacuum, low-temperature STM measurements. Perhaps our results will stimulate groups with such capabilities to look at low-temperature sandwich structures. We have given physically plausible arguments to interpret our results, but clearly more detailed theoretical calculations are needed. Interesting experiments also remain to be done, specifically to the left of Ni or Pd in the transition series, where totally empty s bands are possible but would still allow d hole plasmons and screening.

This work has been supported by various grants from the National Science Foundation, and was made possible by the hard and painstaking work of a number of collaborators, J. C. Lin, N. Shamir, Y.-B. Zhao, and J. E. Whitten, whom it is a pleasure to thank here.

AR950219W

(33) Burdett, J. K.; Sevov, S. *J. Chem. Phys.* **1994**, *101*, 840.

(34) Burdett, J. K.; Mortara, A. K. *Chem. Mater.* **1995**, *7*, 1992.

(35) Whitten, J. E.; Gomer, R. *J. Vac. Sci. Technol.* **1995**, *A13*, 2540.

(36) Note however that "jellium" calculations by N. D. Lang (*Phys. Rev.* **1971**, *B4*, 4234) suggest that for alkali-like overlayer metals almost the bulk work function is obtained after completion of a monolayer.